Canadian Association of Neuropathologists

Abstracts of papers presented at the 33rd Annual Meeting

September 3-5, 1993
Whistler, British Columbia

The 33rd Annual Meeting of the Canadian Association of Neuropathologists was held from September 3rd - 5th, at Chateau Whistler in Whistler, B.C. Local arrangements were made by Dr. K. Berry.

The scientific session consisted of 22 platform presentations, 3 posters and 13 cases for diagnosis. The Royal College of Physicians and Surgeons of Canada speaker was Dr. John D. Steeves, Professor of Neurobiology of the University of British Columbia, Vancouver, B.C. His talk was entitled "Adult CNS Regeneration: Clues from Development". The Jerzy Olszewski lecturer was Dr. Ian Turnbull of the Division of Neurosurgery, University of British Columbia. His talk was entitled "Action Tremor Revisited".

The Association presents two awards annually to trainees/residents giving the best presentations. Dr. Theresa Emory received the Mary Tom Award for her studies of "Intraneural Perineuriomas". Dr. Chunhai Hao received the Morrison H. Finlayson Award for his paper entitled "The Association of Microglia with the Formation of Senile Plaques".

https://doi.org/10.1017/S0317167100049106 Published online by Cambridge University Press

Abstracts of Papers Presented at the 33rd Annual Meeting of the Canadian Association of Neuropathologists

PLATFORM PRESENTATIONS

1.

Familial Erythrophagocytic Lymphohistiocytosis with Extensive CNS Involvement

R.R. HAMMOND and D.A. RAMSAY (La Jolla, U.S.A. and London, Ontario)

This 16 month old female infant presented at 3 months of age with fever, lethargy, jaundice and hepatosplenomegaly, which prompted a differential diagnosis that included a "viral illness", primary liver failure and a storage disease. A liver biopsy narrowed the differential to a "histiocytopathy" because it contained suggestive portal infiltrates. Metabolic screening was negative and the CSF was normal. A left subdural fluid collection was the only abnormality found on head CT scans. She was readmitted at 5.5 months of age with bulging fontanelles, meningismus, irritability, diabetes insipidis and severe anemia. The head CT scan showed no change in the subdural collection but the ventricles were enlarged and the sulci prominent. Cyclosporin was administered on the presumptive diagnosis of "Histiocytosis X". Episodes of sepsis complicated her admission. The CSF was repeatedly sampled and contained scattered lymphocytes and "unusual" macrophages with a protein level as high as 5 g/L. A second liver biopsy allowed the correct diagnosis to be reached.

She subsequently required frequent admissions, usually for the treatment of seizures and intracranial hypertension. At 14 months of age she was admitted for the last time with seizures of increasing severity. She was globally developmentally delayed and quadriparetic. A brain biopsy performed to assess neuroradiologically identified white matter changes showed focal chronic inflammatory infiltrates and microglial proliferation suggestive of a viral encephalitis. She died at 16 months of age after a steady downhill course.

We present the gross and microscopic findings of this case including immunohistochemical and EM examinations. These observations are compared with similar cases described in the literature.

2.

Sudden Infant Death Syndrome: Increased Volume of the Cervical Spinal Cord

J.R. O'KUSKY and M.G. NORMAN (Vancouver, B.C.)

The cervical spinal cord was sampled from 8 sudden infant death syndrome (SIDS) victims and from 8 age-matched control cases without neurological disease (38-46 postconceptional weeks). Morphometric analyses were performed on serial Nissl sections to determine the total volume of the cervical spinal cord from the caudal limit of the cervical enlargement (segment T1) to the spino-medullary junction (segment C1). Individual volumes were also determined for the spinal grey matter, the posterior columns and the anterolateral columns.

The total volume of the cervical spinal cord (in mm^3 as the mean ± standard error) was found to be 917.85 ± 34.95 for control cases and 1175.62 ± 71.08 for SIDS cases. This significant increase in total volume for SIDS cases (28%, $P<0.01$) was not equally distributed between grey matter and white matter compartments. For example, the volume of the spinal grey matter was found to be 333.29 ± 12.31 in controls and 404.54 ± 22.57 in SIDS cases, representing a 21% increase ($P<0.05$). In contrast, the volume of the posterior columns was found to be 187.73 ± 9.35 in controls and 253.75 ± 18.45 in SIDS cases, representing a 35% increase ($P<0.01$), while the volume of the anterolateral columns was found to be 396.84 ± 17.24 in controls and 517.33 ± 33.26 in SIDS cases, representing a 30% increase ($P<0.01$). The cross-sectional areas of the white matter columns were determined at levels C1 and T1 (in mm^2 as the mean ± standard error). The cross-sectional areas of the posterior columns were significantly greater in SIDS cases than in controls, both at level C1 (7.780 ± 0.375 versus 5.858 ± 0.224, $P<0.001$) and at level T1 (4.688 ± 0.255 versus 3.679 ± 0.189, $P<0.01$). Similarly, the areas of the anterolateral columns were significantly greater in SIDS cases, both at lever C1 (13.356 ± 0.783 versus 10.962 ± 0.408, $P<0.05$) and at level T1 (10.837 ± 0.560 versus 8.693 ± 0.427, $P<0.01$). There was a significant correlation between spinal cord volume and brain weight for both SIDS cases and controls. However, correlations between volume and postmortem interval were not statistically significant for either group. In several additional cases, electron microscopy of selected nuclei in the brainstem and spinal cord revealed no detectable signs of edema or gliosis.

The increased volume of the cervical spinal cord in SIDS cases is consistent with previous reports of increased brain weight and increased volume of the medulla in SIDS, suggesting a developmental disorder of the brainstem and spinal cord.

Supported by the Medical Research Council of Canada.

3.

Cytogenetic Analysis of 109 Pediatric CNS Tumors

ETELA NEUMANN, DAGMAR K. KALOUSEK, MARGARET G. NORMAN and PAUL STEINBOK (Vancouver, B.C.)

Reports of cytogenetic abnormalities in pediatric central nervous system tumors are important for collecting and comparing large numbers of karyotypes of primary CNS neoplasms to produce statistically significant correlations. We report cytogenetic results of 119 samples of pediatric CNS tumors from 109 patients. Tumors included 33 low grade astrocytomas, 18 high grade astrocytomas, 14 gangliogliomas, 13 ependymomas, 17 primitive neuroectodermal tumors (PNET), 3 choroid plexus papillomas and carcinomas and miscellaneous group of twenty

rare primary CNS tumors and metastases. Cytogenetic results were correlated in each group with histological subtype and survival. The study indicated specific chromosomal abnormalities in different groups of tumors. Low grade astrocytomas showed mostly numeric abnormalities with gains of chromosome 7, high grade astrocytomes showed differences from karyotypic changes seen in adults in lacking double minutes and monosomy 10. The ependymoma group showed the largest proportion of abnormal karyotypes with frequent involvement of chromosome 6 and 16. Chromosome 6 was the single most common abnormal chromosome in this study closely followed by chromosome 1 and 11.

We conclude that pediatric CNS neoplasms differ from adult tumors cytogenetically as well as histologically and biologically.

4.

Dysplasia and Hyperplasia of Periventricular Germinal Cells: Absence of Cerebral Ventricles

CHENG-MEI SHAW and ELLSWORTH C. ALVORD, JR. (Seattle, U.S.A.)

To our knowledge, complete absence of cerebral ventricular cavities has not been previously described as an entity of CNS malformation. Markedly disorganized maldevelopment of the deep cerebral nuclei and moderately disorganized maldevelpment of the cerebral cortex were observed in the brains of a 3-year-old girl and a male newborn infant. One showed complete and the other showed partial obliteration of the lateral and third ventricles. Both showed severe maldevelopment of the basal ganglia which were represented by a large central mass consisting of multiple nodules of grey matter without any discernable differentiation into lenticulostriate nuclei, thalamus or hypothalamus. Minor malformations involved the cerebral cortex, cerebellum and mesencephalon to varying degrees. Each case was thought to be unique and different until a brain of a fetus of 155 days gestation was studied. This fetal brain showed exuberant and disorganized periventricular extension of germinal matrix cells with obliteration to the lateral and third ventricles. It was concluded that hyperplasia and disorganized migration of the periventricular germinal matrix in the second trimester caused severe maldevelopment of the deep cerebral nuclei in the two previous cases.

5.

Neurofibrillary Tangles in Niemann-Pick Disease Type C

K. SUZUKI, C.C. PARKER and P.G. PENTCHEV (Bethesda, U.S.A.)

Niemann-Pick disease type C (NP-C) is an autosomal recessive lipidosis characterized by a defect in cellular trafficking of exogenous cholesterol resulting in a lysosomal accumulation of unesterified cholesterol. NP-C is biochemically distinct from the primary sphingomyelin lipidosis (Niemann-Pick disease type A & B). The clinical manifestations of the NP-C are heterogeneous. We recently examined the brain of three patients with NP-C, in which numerous neurofibrillary tangles but no amyloid or neuritic plaques were noted. One of the patients was a 37-year-old male. Shortly after birth he had neonatal jaundice and hepatomegaly. Since age 10, he was noted to have slow but progressive mental deterioration, ataxia, slurred speech, facial tics, dysarthria, facial grimacing and a vertical supranuclear gaze palsy. Neuropathological examination revealed an atrophic brain with swollen storage neurons throughout. In addition, Bielschowsky stain revealed numerous neurofibrillary tangles throughout cerebrum and brainstem. The tangles tended to be more numerous in the areas where swollen neurons were most conspicuous. However, neurons with neurofibrillary tangles were not always swollen. The tangles were particularly pronounced in the hypothalamus, orbital gyrus, cingulate girus, hippocampus and entorhenal cortex. Occasional neurofibrillary tangles were noted in the basal ganglia and thalamus, the fascia dentata, inferior olives and spinal gray matter. The second patient was a Hispanic female whose onset of the disease was around eight years of age with difficulty in school word and progressive ataxia. Gradually, she developed dystonia, dysarthria, ataxia and typical vertical supranuclear gaze palsy. She died at age 18. Her brain showed numerous storage neurons. Neurofibrillary tangles were seen in the perikarya as well as within meganeurites of neurons in the entorhenal cortex. Third patient, a female who developed clinical symptoms in her 20s, revealed numerous neurofibrillary tangles in the hippocampus, entorhenal cortex and hypothalamus. A few tangles were also noted in the orbital gyrus. Neurofibrillary tangles have been noted by others in some NP-C cases (Horoupian & Yang, 1978; Curry, personal communication) but, to our knowledge, not in other types of lipidosis. Thus, it appears that neurofibrillary tangles may be a unique manifestation of neuronal cytoskeletal abnormalities in the NP-C. Whether neurofibrillary tangles are present only in certain clinical sub-group of NP-C is yet to be studied.

6.

Potential Volume-Doubling Times of Gliomas Defined by Flow-cytometry and Immunocytochemistry (%Cycling Cells)

ELLSWORTH C. ALVORD, JR. (Seattle, U.S.A.)

On a nomogram which reveals the mathematical relationships between S-phase fraction and growth fraction (GF) one can define the potential tumor volume-doubling time (Tp) of any neoplasm. From serial scans one can define the actual tumor doubling time (Td) and then calculate the cell loss factor ($\Phi = 1 - Tp/Td$); but, of course, one would like to do the reverse, determine the cell loss factor and define the actual doubling time. Since this last is not yet possible, one must be content with collecting data on gliomas and seeing how the predicted doubling time correlates with survival. Our first 2 dozen gliomas show a reasonable separation in potential doubling times, as follows:

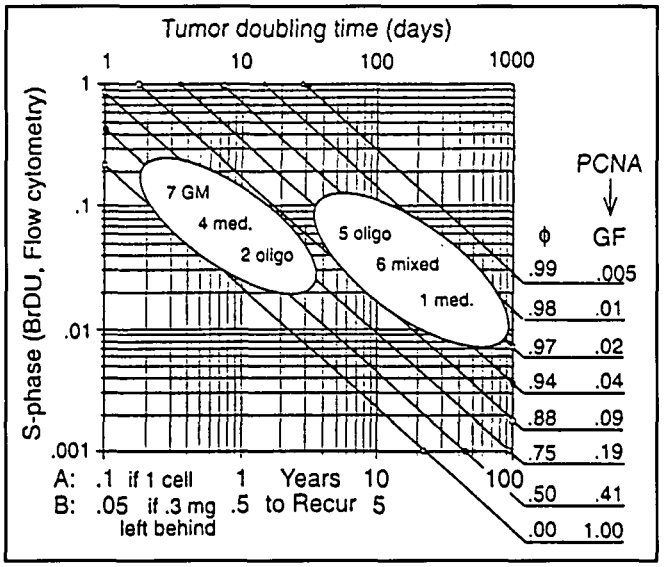

7.

Hemangioblastoma, Ultrastructure and Immunohistochemistry of Stromal Cells

B. LACH, A. GREGOR, P. RIPPSTEIN and A. OMULECKA (Ottawa, Ontario and Lodz, Poland)

In order to resolve continuing controversy on histogenesis of stromal cells (SC) of hemangioblastoma (HMB), immunohistochemical, ultrastructural and immunoelectron microscopic properties of these cells were studied in 40 cases of HMB. Immunohistochemistry demonstrated S-100, NSE and vimentin (VIM) reactions in all SC. Few cases contained SC positive for desmin, factor VIII (FVIIIAg), Ulex europaeus communis lectin (UE), GFAP and factor XIIIa. However, the overwhelming majority of SC was negative for the above antigens as well as for other markers indicating either neuroendocrine, endothelial (EC), smooth muscle or histocytic differentiation. Proliferating cell nuclear antigen (PCNA) and K67i immunoreactive was found in EC and SC indicating proliferation of these cells in HMB.

Electron microscopy of 14 tumours demonstrated several SC types, with features of modified EC, pericytes and smooth muscle cells, and their intermediate forms. All tumours contained undifferentiated mesenchymal cells, often closely associated with SC. Few SC were found within capillary lumina in contact with EC. Groups of SC formed slit cavities closed by intercellular junctions or intercellular caveolae, both reminiscent of the early vascular lumina seen in normal vascularization. A very few SC could be classified as lipidized astrocytes, smooth muscle cells and macrophages. Post-embedding immunoelectron microscopy (3 cases) showed FVIIIAg in Weibel-Palade bodies (WPB) in EC lining the tumour vessels. However, some endothelial WPB, were FVIIIAg negative. SC contained only FVIIIAg-negative WPB. This finding may explain negative results for markers of EC differentiation in SC, despite the morphological evidence of their endothelial nature.

It is concluded that SC represent a hetereogeneous population of abnormally differentiated cells of angiogenic lineage, with features of modified EC, pericytes and/or smooth muscle cells, and their intermediate forms. The development of SC in HMB could be related to proliferation of angiogenic mesenchymal cells, and at the same time, their inability to develop capillary lumina integrated with the vascular network of the tumour.

8.

Quantitative Morphometric Image Analysis in Human Astrocytomas

M.K. RAHIMIAN, B.H. LIWNICZ and R. BOWMAN (Loma Linda, U.S.A.)

Morphometric image analysis of cytological features was performed on astrocytomas using Cell Analysis System (CAS 200). Diffuse astrocytomas grade II-IV were analyzed. In addition, pilocytic astrocytomas, designated grade I were studied. Nine cytological features were evaluated of which six were selected as significant. Discrimination analysis was performed on these six cytological parameters and their standard deviations, making a total of 12 variables. Discriminant analysis resulted in correct cytological classification of 92% of cases ($p<0.04$ for all significant parameters). Stepwise discrimination analysis resulted in correct classification of 80% of cases. When grades I and II, and grades III and IV were grouped together, 96% of cases showed correlation between histological and CAS-derived classification with and without stepwise function ($p<0.04$ for all parameters). In addition to nuclear counts and nuclear size, the cell size, cytoplasm size, and cytoplasm shape significantly contributed to discriminated functions. The results suggest that morphometric image analysis discriminates between grades of astrocytomas. In cases where only very small samples, not allowing for precise histological evaluation, are available, grades I and II should be combined and diagnosed as low grade astrocytomas and grades III and IV as high grade astrocytomas based on CAS evaluation.

9.

Adult Onset of Neurological Involvement in a Patient with Glycogenosis IV Treated with Tedral^{R}

E.S. JOHNSON and A.B. JONES (Edmonton, Alberta)

Glycogenosis IV (branching enzyme deficiency) is characterized by hepatic deposition of an amylopectin-like polysaccharide with ensuing cirrhosis, and is inevitably fatal before puberty. CNS involvement may occur in early childhood. This report, however, documents the exceptionally long survival of a 21-year-old woman, who was diagnosed at age 21 months, has been treated since that age with ephedrine/theophylline/phenobarbital (Tedral^{R}) (as a glycogenolytic agent) and recently presented with a history of 6 months' duration of neurological dysfunction: increasing difficulty maintaining balance, wide-based gait, positive Rhomber's sign. She concurrently complained of proximal muscle weakness. Liver biopsies in early childhood showed marked deposition of an abnormal polysaccharide within hepatocytes with concomitant cirrhosis. This material resembled amylopectin ultrastructurally and showed a spectrographic

https://doi.org/10.1017/S0317167100049106 Published online by Cambridge University Press

absorption starch/iodine peak at 505 nm, consistent with long chain unbranched glycogen. Histochemical studies were further characteristic: strong PAS positivity with relative resistance to digestion by diastase and pectinase, and tinctorial affinity for aldehyde fuchsin and alcian blue pH 2.5. Diagnosis was confirmed by deficiency of brancher enzyme couped to both phosphorylase and glycogen synthase in fibroblast cultures. Liver biopsies in later childhood, after treatment had been started, and in adolescence revealed decreased amounts of stored polysaccharide and loss of staining affinity for aldehyde fuchsin and alcian blue. Deposition of an amylopectin-like substance with similar histochemical properties was demonstrated within astrocytes in the cortex and subcortical white matter of a frontal brain biopsy at age 21 years. By electron microscopy this material consisted on non-membrane bound, globular masses of sparsely branched, 5.5 - 6.7 nm filamentous profiles swirling around a flocculant electron dense granular core. Variable amounts of similar material were present in temporalis and quadriceps muscle biopsies. This case is notable for the extraordinary longevity of this patient with type IV glycogenosis, which correlates with the altered histochemical properties and diminished hepatic deposition of the abnormal glycogen, possibly mediated by Tedral^{R} therapy. Nonetheless involvement of the brain and muscle occurred as described in fatal juvenile case, albeit considerably delayed. Successful liver transplant has been performed.

10.

Features of the Eosinophilia Myalgia Syndrome in a Mouse Model

HERBERT MANZ, CAROLYN BLANK, MARIELLA TEFFT, ROBERT SEARS, LARRY MOSCOWITZ, JOHN MARENCO, PAUL KATZ and DANIEL CLAUW (Washington, U.S.A.)

The Eosinophilia Myalgia Syndrome (EMS) is a multisystem connective tissue disease characterized by initially high peripheral eosinophil count, severe myalgia, and various neurologic, pulmonary, and cutaneous features. Epidemiologic studies have suggested that most EMS patients were consuming L-tryptophan (LT) manufactured by a single company. The Centers for Disease Control has identified 6 compounds in LT that are present in higher concentrations in case-associated lots (CALT); 2 of these have received the most attention, 1,1'-[ethylidenebis]-tryptophan (EBT) and 3-[phenylamino]-alanine (PAA). There have been numerous attempts to develop an animal model of EMS using EBT and CALT (but not PAA), but none have displayed the hallmarks of the disease, namely inflammation of fascial and perimysial areas, and eosinophilia.

We began with ninety 4-week old female C57 black mice. Half (Group A) were fed a normal diet, and half (Group B) were fed a pelleted diet containing 5x the normal concentration of Sigma LT. Each of these groups was further divided into 4 subgroups which received daily IP injections of: 1) saline, 2) 1.07 mcg EBT, 3) 0.72 mcg PAA, 4) both EBT and PAA (at the same doses). At sacrifice 3 and 8 wks later, a CBC was performed, and full-thickness samples of skin with trapezius or femoral muscle group were obtained; the heart was also examined. The coded tissue specimens were randomized and read by the neuropathologist; the degree of inflammation in each specimen was scored from 0 (not present) to 4 (severe). At all but 1/8 data points, the mean peripheral eosinophil count was higher for all of the groups which received PAA than the A1 control group, but this did not reach statistical significance. Multifactor ANOVA analysis was performed. At 3 weeks, there were generally no statistically significant dietary or drug effects. At 8 weeks, the high LT diet was associated with significantly increased inflammation in the superficial adipose (p=.0001), deep adipose (p=.0085) and muscle (p=.021) layers in the trapezius, muscle only (p=.0035) in the femoral region, and in the heart (p=.007). PAA was independently associated with increased inflammation in the trapezius muscle and heart (p=.001, .016). EBT led to increased inflammation only in the heart (p=.021). These data suggest that a high LT diet and PAA have the greatest influence on the development of EMS-like changes in skeletal muscle and connective tissue.

11.

Progressive Oral-Mandibular-Lingual Dyskinesia and "Mosaicism" of the Neostriatum

KEVIN D. BARRON and STEWART A. FACTOR (Albany, U.S.A.)

This clinico-pathological report concerns a man hospitalized in psychiatric institutions repeatedly from 1960-68. Diagnoses included low IQ, paranoid schizophrenia and major depression. He was treated with neuroleptics until 1968. In 1967, he had onset of a movement disorder characterized by craniocervical dystonia, blepharospasm, oculogyric crises and oral-mandibular-lingual movements. Dysphagia and dysphonia were concomitants. He died in 1992 at age 50.

Coroner's autopsy showed occlusion of the pharynx and larynx by a food bolus. The general autopsy was otherwise unremarkable. The brain had a normal macroscopic appearance. Microscopically, the caudate nucleus and the putamen were hypomyelinated and their neuropil was traversed by interlacing, amyelinated, broad, cellular strands that contained both neurons and neuroglia. The former had a usual histological appearance. The latter were predominantly large, fiber-rich astrocytes. These stained intensely by Holzer and immunohistochemical (GFA) methods. Intense astrocytic staining highlighted the interweaving cellular strands conferring on the caudoputamen a mosaic-like appearance at low power magnifications. The islands of striatal neuropil between the cellular strands had a usual appearance except for a suspected reduction in large neuron density. The pallidum showed mild nerve cell loss and hypomyelination. The remainder of the brain was normal except for slight neuronal loss and astrogliosis in the CA4 region of the hippocampus bilaterally.

A similar disorder (Lubag) has been described in two autopsied Filipino patients (Altrocchi and Fornio, 1983; Waters *et al.*, 1992) and appears to be an X-linked recessive form of extrapyramidal disease. An autopsied case in a non-Filipino male (Gibb *et al.*, 1992) also received neuroleptic medication but only after the onset of a dystonic syndrome. The mosaic appearance of the basal ganglia described for Lubag would not appear to be specific for that disease. Our case represents the fourth autopsied patient with "mosaicism" of the caudoputamen

and an extrapyramidal syndrome of dystonic nature. Administration of neuroleptics does not appear to relate to this condition. The plump, eosinophilic somas and abundant fibrillary processes of the reactive astrocytes of our case seemed to indicate an astrocytic reaction initiated much more recently than the many years of clinical involvement would have led one to anticitpate.

12.

The Association of Microglia with the Formation of Senile Plaques

C. HAO, I.R.A. MACKENZIE and D.G. MUNOZ (London, Ontario)

Microglia are immunocompetent cells involved in inflammatory processes in the CNS. The association of microglia with senile plaques (SP) in Alzheimer's disease (AD) has led some researchers to hypothesize that the microglia are the amyloid-producing cells. Others have taken the broader view that general inflammatory mechanisms may be involved in the formation of SP and the pathogenesis of AD. It is commonly accepted that SP may evolve through several stages, starting with non-amyloid containing diffuse plaques (DP) to neuritic plaques (NP) composed of both amyloid and dystrophic neurites to full-blown AD. The present study is designed to examine the role of microglia in this process.

We evaluated the density of microglia in the temporal neocortex of 30 non-demented individuals (12 without any SP, 18 with DP only and 10 with both DP and NP) and 16 patients with typical AD. Microglia were identified on formalin-fixed paraffin-embedded tissue sections using a lectin, *Ricinus communis agglutinin-1 (RCA-1).* The SP were demonstrated by anti-beta-A4 immunohistochemistry and modified Bielschowsky's silver stain. We found no significant difference in the mean density of microglia among the three groups of non-demented patients; 33 ± 22/mm^2 in SP-negative cases, 35 ± 20/mm^2 in DP-positive cases and 30 ± 12/mm^2 in the cases with both DP and NP. The mean density of microglia in the 16 AD cases, however, was 78.7 ± 23/mm^2, which was significantly different from each of the other groups ($p<0.01$). Our results indicate that the presence of DP and NP is not associated with an increase in the density of microglia and, therefore, inflammatory mechanisms are unlikely to play a role in SP genesis. The proliferation of microglia seen in AD may represent a reaction to the presence of extensive pathologic changes.

13.

Changes of Alzheimer's Disease in the Brain of a 46-year-old Man with Myotonic Dystrophy

JACQUES B. LAMARCHE, FRANÇOIS EVOY and BERNARD LEMIEUX (Sherbrooke, Quebec)

Alzheimer's neurofibrillary tangles without senile plaques have been recently described in the brain of seven Japanese patients aged 35 to 56 years affected with myotonic dystrophy. (Acta neuropathol 82:1-5, 1991) We report the association of the classical clinical form of myotonic dystrophy with the histological changes of Alzheimer's disease in a 46-year-old French Canadian man who died suddenly presumably from a cardiac conduction defect. The patient was mildly mentally retarded with no recent documentation of cognitive deterioration. He belonged to a large family suffering from myotonic dystrophy which has been genetically investigated by indirect DNA analysis and more recently by direct DNA analysis (CTG repeat expansion).

At autopsy, the brain weighed 1250 g and there was no cortical cerebral atrophy. Microscopic examination revealed a small number of hippocampal neurons with granulovacuolar degeneration, neurofibrillary changes and Hirano bodies. In the parahippocampal gyrus, numerous neurons showed neurofibrillary tangles. In the neocortex, the tangles were sparse but there were up to 10 diffuse senile plaques per sq mm.

No definite association of myotonic dystrophy and Alzheimer's disease has been reported clinically or morphologically and our case could be a fortuitous occurrence. However, because the gene of myotonic dystrophy has been localized on band 19q13.3 and linkage studies in familial Alzheimer's disease of late onset have suggested some evidence for chromosome 19 linkage, our findings could be a significant clue leading to the identification of the exact location of the gene of Alzheimer's disease of late onset. As the finding of other similar cases is susceptible to facilitate the genetic studies of Alzheimer's disease of late onset, one should systematically search for morphological as well as clinical evidence of Alzheimer's disease in all cases of myotonic dystrophy.

14.

Changes in Peptidergic Neurons of the Subcortical White Matter in Alzheimer's Disease

L.C. ANG and D. SHUL (Saskatoon, Saskatchewan)

The term "interstitial cells" has been used by Cajal (1911) to describe cells with neuronal morphology in white matter of mice cerebrum. Subsequently, Golgi studies combined with electron microscopy confirm that these cells are neurons (Kostovic and Rakiv, 1980). In the adult rat and human cerebrum, these interstitial neurons have been shown to contain GABA, somatostatin (SS) and neuropeptide Y (NPY) (Schmechel *et al.*, 1984, Hendry *et al.*, 1984, Sorensen 1982, Davies *et al.*, 1990). Although their functions are uncertain in humans, in adult rats these neurons project to overlying cortex and also to other cytoarchitectonic areas suggesting that they may play an important role in maintenance of normal cerebral cortical circuitry. We have studied the subcortical neurons in the striate cortex form 8 Alzheimer patients (mean age 73.8 yrs ± 11.17) and 8 age matched neurologically normal patients (mean age = 72.6 yrs ± 8.73). Frozen 50 μ sections were immunostained individually with one of the following antibodies: substance P (SP), cholecystokinin (CCK), SS and NPY using the ABC technique and then counterstained with luxol fast blue to highlight the white matter. The immunostained neurons were counted only in subcortical areas delineated and measured by the Bioscan Optimas image analyzer. The results reveal CCK

immunoreactive (ir) neurons are very scarce both in control and Alzheimer subcortical white matter. While there are slight decrease in SS ir and NPY ir subcortical neurons in Alzheimer brains, there is considerable overlap with controls. The most significant finding is the definite decrease in density of SP ir subcortical neurons in Alzheimers disease (mean 0.20/mm^2) compared to control (mean 2.46/mm^2).

15.

Cumulative Dose-Response Induction of Neurofilamentous Degeneration Following Chronic Aluminum Exposure *In Vivo*

S. GAYTAN-GARCIA, D.M. JAKOWEC and M.J. STRONG
(London, Ontario)

To further define the chronic aluminum-induced progressive myelopathy model of human motor neuron degeneration, we have temporally correlated the degree of neurological impairment with the topographic distribution of neurofilamentous degeneration following monthly intracisternal inoculums of either 100 µg $AlCl_3$ in 0.9% NaCl (n=22) or 0.9% NaCl alone (n=8) in young adult New Zealand white rabbits. Rabbits were examined weekly and assigned a clinical score based on the degree of neurological deficit, killed at intervals, and the extent of neuropathological degeneration quantified by an observer blinded to the treatment interval. Control rabbits remained unaffected while the remaining developed increasing degrees of limb splaying, hyperreflexia, gait abnormalities, paraspinal hypotonia, and impaired tonic immobility responses. At day 51 (n=5), fusiform neuroaxonal distention within the ventral spinal cord was observed, with neurofilamentous degeneration rarely observed within the brainstem. Spinal motor neurons were otherwise spared. By day 107 (n=6), spheroid formation was additionally observed, within the ventral spinal cord, while neurofilamentous degeneration was rarely evident in the subiculum, parasubiculum, and medullary nuclei. By day 156 (n=6), rare anterior horn cell chromatolysis with early ventral horn gliosis was apparent as was diffuse neurofilamentous degeneration within the subiculum, parasubiculum, superior colliculus, and medullary nuclei, with cerebellar torpedo and empty basket cell formation evident. By day 267 (n=5), neuropathological changes were noted throughout the neuroaxis. Perikaryal neurofilamentous inclusions demonstrated a robust immunoreactivity to monoclonal antibodies recognizing poorly phosphorylated NFH isoforms (SMI 32) by day 107 whereas neuroaxonal spheroids demonstrated only faint SMI 32 immunoreactivity regardless of disease duration. In contrast, neuroaxonal spheroids were intensely immunoreactive to antibodies recognizing highly phosphorylated NFH isoforms and an age-dependant phosphorylation state (SMI 34) by day 107. A similar pattern of immunoreactivity was observed in perikaryal inclusions, maximal by day 267. Ubiquitin immunoreactivity appeared only after neurofilamentous aggregates had formed.

These observations indicate a cumulative response to repetitive, intracisternal inoculums of $AlCl_3$ that correlates with the degree of clinical deficit. While the anterior horn cells and descending supraspinal nuclei are preferentially involved, more disseminated neuropathological changes are evident.

Supported by grants from the ALS Society of Canada, Upjohn London Neurosciences Program and the Medical Research Council of Canada (MJS).

16.

Recovery in Aluminum-Induced Chronic Motor System Degeneration: Clinicopathological Correlates

M.J. STRONG, S. GAYTAN-GARCIA and D. JAKOWEC
(London, Ontario)

We have studied the potential for recovery following the induction of a chronic, progressive myelopathy induced in young adult New Zealand white rabbits. Following intracisternal inoculums of 100 µg $AlCl_3$ administered every 4 weeks, rabbits develop perikaryal and neuritic neurofilamentous inclusions predominantly within the spinal motor neurons and nuclei of the descending supraspinal pathways in a dose-dependant fashion that correlates with the degree and severity of neurological deficits. At intervals of 51, 107 and 156 days, randomly selected rabbits were either withdrawn from further inoculums and allowed to survive until the termination of the study (day 265), or killed and morphometric measures of the extent of neurofilamentous aggregate formation quantified, or allowed to continue to receive monthly inoculums. Control rabbits, inoculated with 0.9% NaCl remained clinically and neuropathologically unaffected. A total of 39 rabbits were studied. All rabbits developed a progressive myelopathy manifested by gait abnormalities, limb splaying, impaired tonic immobility responses, hyperreflexia and muscle wasting. At each of the intervals, no significant difference in the degree and severity of clinical deficits was observed between those rabbits continuing to receive $AlCl_3$ and those being removed from the study.

By day 267, those rabbits withdrawn at days 56 and 107 were clinically indistinguishable from control rabbits, while those withdrawn at day 156, although severely afflicted at the time of cessation of $AlCl_3$ inoculation, had only minimal neurological deficits. By day 56, no significant pathological changes were observed, either in the treated group or in those allowed to survive. However, in the remaining groups, a significant reduction in the number of neurofilamentous inclusions was observed in those rabbits allowed to survive. By day 107, inoculated rabbits demonstrated neuroaxonal distention and axonal spheroids within the ventral horns, and perikaryal inclusions in 12 and 30% of motor neurons (cervical and lumbar, resp.). In those surviving without further aluminum exposure, only rare neuroaxonal distention was observed and no cells demonstrated perikaryal inclusions. By day 156, extensive neuroaxonal distention and spheroid formation was observed, with 33 to 48% of spinal motor neurons (cervical and lumbar, resp.) developing perikaryal inclusions. In those allowed to survive, 7 and 3% of neurons continued to have pathology, while only a mild degree of neuroaxonal distention and spheroid formation persisted.

These observations suggest a significant potential for recovery from both the clinical and neuropathological lesions induced by chronic, repetitive low dose $AlCl_3$ inoculums. We propose that this model of combined upper and lower motor neuron degeneration will provide a valuable adjunct in the study of amyotrophic lateral sclerosis.

17.

"Intraneural Perineurioma": A Clonal Neoplasm Associated with Abnormalities of Chromosome 22

T.S. EMORY, B.W. SCHEITHAUER, M.B. WOOD, B.M. ONOFRIO and R.B. JENKINS (Rochester, U.S.A.)

The nature of perineurioma, variably termed "localized hypertrophic neuropathy, intraneural neurofibroma and hypertrophic interstitial neuritis" has long been an issue of contention. Although some consider it a neoplasm, recent studies favor a reactive process, perhaps due to repeated trauma with associated loss of integrity of blood-nerve barrier. The latter has experimentally been shown to result in the proliferation of perineurial cells. Six clinically and morphologically typical perineuriomas were studied by histologic, immunochemical and ultrastructural methods; one was subject to tissue culture and cytogenetic analysis and another to fluorescence *in situ* hybridization (FISH). The patients, 3 males and 3 females, ranged from 12 to 38 years in age. All tumors were intraneural and involved extremities. Neuropathic symptoms, motor in all cases and sensory in 3, were present for 8 months to 7 years (mean 2.5 years). Symmetric, fusiform, segmental nerve enlargement, was evident in 5 (6) patients. No association with a phakomatosis was noted. Treatment consisted of biopsy in 4 and resection in 2 cases. Histologically, most of the epithelial membrane antigen-reactive, S-100 protein-negative perineurial cells surrounded myelinated or nonmyelinated nerve fibers, some with accompanying S-100 protein-positive Schwann sheaths; some whorls lacked a central axon. A single mitosis was noted in 1 case. The MIB-1 antigen labelling index ranged from 4-17%. Staining for p53 antigen showed no (2/6), rare (2/6), or scattered (2/6) immunoreactive nuclei. Cytogenetic analysis of one case demonstrated a chromosomally abnormal clone: all metaphase cells were abnormal such that the tumor cells appeared to be homozygously deficient for the region 22q11.2->qter. In another case, 53% of interphase nuclei had three FISH signals with the chromosome 14/22 probe, suggesting either monosomy for the centromere of chromosome 14 or the centromere of chromosome 22. On the basis of this study we conclude that a) perineurioma represents a clonal neoplastic rather than a reactive process, b) despite their slow growth, rare mitoses and proliferation indices attest to ongoing cell multiplication, c) most are localized and self-limited, but occasional examples show extensive intraneural spread, d) the observed cytogenetic abnormalities suggest that a gene on chromosome 22 may play a role in the pathogenesis of perineurioma and also suggests that the pathogenesis of perineurioma is similar to other nerve sheath tumors, and e) alterations in the tumor suppressor gene p53 may play a role in the genesis or continued growth of perineuriomas. The spectrum of perineurial cell neoplasms must be expanded to include not only rare, extraneural soft tissue tumors, but intraneural perineurioma as well.

18.

Long Term Primary Culture of Human CNS Tissue in Serum-free Conditions

R.R. HAMMOND, C.L. ACHIM, E. MASLIAH, D.A. PETERSON, C.A. WILEY and F.H. GAGE (La Jolla and Pittsburgh, U.S.A.)

Three dimensional CNS cell aggregates have been previously reported as an additional method of cell culture to the me traditional monolayer and organotypic slice techniques. We are expanding of these efforts to demonstrate the utility of long term primary CNS cell aggregates (brain microspheres) maintained in serum-free conditions in the study of human neurodegeneration.

Human cerebral tissue obtained from second trimester abortuses has been dissociated into a single cell suspension and allowed to reaggregate into microspheres. Characterization of the brian microspheres reveals a mixture of glial and neuronal cells which remains stable over time (some cultures have been observed for more that 4 months). Upon plating onto substrate-coated culture ware, adherence of the spheres is followed by extension of neuronal and glial cell processes and outward cellular migration. A variety of neuronal markers can be identified including neurofilament (NF), neuron specific enolase (NSE), amyloid precursor protein (APP), growth associated protein (GAP43), microtubule associated protein (MAP2), synaptophysin (SY38) and synaptotagmin (SV48). NF, NSE and MAP2 positivity are present in the cell body and processes while APP, GAP43, SY38 and SV48 show a more punctate pattern with a membranous distribution highlighting neuronal processes.

Immunocytochemical and cytoarchitectural details were demonstrated at a higher degree of resolution with confocal laser microscopy and scanning electron microscopy (EM). We are in the process of examining the tissue by transmission EM.

This system supports neuronal survival and differentiation in an *in vitro* environment that resembles human CNS neuropil. The characterization to date gives a framework upon which neurotoxins or infectious agents could be examined for their neurodegenerative potential. Likewise, it allows for the evaluation of the positive influences of neurotrophins, differentiating agents and extracellular matrix molecules.

19.

Rosenthal Fibers, Immunoelectron Microscopic, Spectroscopic and Biochemical Analysis

B. LACH, P. RIPPSTEIN, M. SIRKORSKA, I. DEBELL, P. WONG and A. GREGOR (Ottawa, Ontario)

Composition of Rosenthal fibers (RF) in 17 gliomas and in the RF-enriched brain fractions (RFf) from Alexander's disease and optic glioma, was studied by an immunohistochemistry (PAP), Western blot technique (WBT), immunoelectron microscopy (IEM) and infrared spectroscopy (SPC). PAP localized ubiquitin (UB), glial fibrillary acidic protein (GFAP) and vimentin (VIM) as rings of overlapping reactions around negative RF "cores". Many RF were entirely negative for UB as well as for intermediate filaments (IF).

Immunoelectron microscopic (IEM) localization of UB, VIM, α B-crystallin (CR) and GFAP was performed on selected tumours and RFf. UB was found in all RF and on intermediate filaments (IF) around RF. GFAP and VIM reaction was present on IF, including those trapped within RF. In addition, the granular and amorphous components of RF were also GFAP-positive. Neither GFAP- nor UB-negative RF were seen in IEM. However, scattered RF were negative for CR, considered to be an essential component of every RF. Come cells with RF contained lysosome-like inclusions with material similar to RF and

reactive for UB. This finding suggests that the lysosomes of astrocytes may degrade ubiquitinated components of RF.

RF fractions were analyzed by WBT for GFAP, VIM, UB and CR. RFf contained proteins that were recognized by anti-GFAP, anti-VIM, anti-CR and anti-UB sera. RFf displayed multiple bands of GFAP- and UB-positive protein subfractions. Only small amounts of native and ubiquinated CR was found. VIM appeared to be present only as an unaltered and not ubiquinated single band.

SPC indicated that formation of RF is accompanied by conformational change of proteins, due to strong hydrogen binding between amino groups and macroaggregations of protein molecules, similar to changes seen in Mallory bodies in the liver.

It is concluded that RF formation is associated with ubiquination of GFAP and many GFAP-positive protein subfractions of different molecular weight, leading to their macroaggregation and entrapment of other astrocytic proteins such as CR and VIM.

20.

CNS Coccidioidomycosis

P.S. MISCHEL and H.V. VINTERS (Los Angeles, U.S.A.)

Coccidiodes immitis is a dimorphic fungus endemic to the Southwest United States, Central and South America. Infection is usually subclinical or a self-limited pulmonary infection. However, 0.5 percent of those infected go on to develop disseminated disease, sometimes involving the CNS. Epidemiologic data show a significant increase in new cases of Coccidiodes infection since June of 1991, with an increase in disseminated disease. Immunosuppression, including Acquired Immunodeficiency Syndrome (AIDS), is a major risk factor.

We present the case of a 30-year-old Hispanic male with AIDS who developed cough, fever, nigh sweats, headache, right facial and upper extremity weakness and confusion. CSF showed a glucose of 28 mg/dl, a protein of 187 gm/dl, 40 rbc/cmm and 80 wbc/cmm (67% PMNs and 33% monocytes). Gram stain, AFB, cytology, VDRL, Cryptococcus antigen and Coccidiodes antibody were negative in the CSF. A presumptive diagnosis of Tuberculous meningitis was made, and the patient was started on appropriate medication. His symptoms worsened and he expired three weeks later. At autopsy, he was found to have disseminated *Coccidiodes immits* infection with extensive involvement of the central nervous system including meningitis, encephalitis and myelitis. Widespread involvement of the brain parenchyma with granulomata/abcesses and an associated endarteritis obliterans were noted. Review of archival records at UCLA-CHS showed 15 previous cases of disseminated coccidiodomycosis in a clinically heterogeneous group of patients, nine of whom demonstrated CNS involvement. CNS coccidiodomycosis can present with a variety of neurologic symptoms of varying severity.

21.

Neuropathological Criteria for the Diagnosis of Vascular Dementia

BARRY REWCASTLE and IRMA PARHAD (Calgary, Alberta)

Encouraged by Health and Welfare Canada, the Canadian Study of Health and Aging was established in 1989. It consists of a network of Canadian centres based on the Department of Epidemiology at the University of Ottawa and linked to the Federal Laboratory Centre for Disease Control with further links to the Consortium to Establish A Registry for Alzheimer's Disease (CERAD) and to the World Health Organization (WHO) five country study of dementia. The objectives were to establish Canadian Data on dementia and to determine prevalence, risk factors, and the assessment of caregiver burden and evaluation of intervention programs. Extending from the latter was developed the Consortium of Canadian Centres for Clinical Cognitive Research (C5R). This presentation is directed to Canadian Neuropathologists to make them aware of this initiative and to seek their collaboration in developing a uniform approach to the neuropathology study of any patient identified through the C5R with possible vascular dementia. Specific questions to be addressed include how large must a single infarct be to produce dementia, what structures must be destroyed or specific system connections interfered with, does a single infarct result in progressive intellectual deterioration. If multiple, which infarctions are significant, and the ages of lesions. If no obvious infarctions are identified by imaging, the determination of the nature of the vascular disease and documentation of vessel involvement. Finally, a correlation of the clinical, pathological and in-vivo and post-mortem imaging data will be made. The following criteria are suggested for protocol development and discussion and include identification of vascular damage through post-mortem imaging, number, location, volume of tissue damage and determination of etiology. Assessment of nonvascular damage i.e., aging, Alzheimer's Disease or other neurodegenerative disorders would follow and thereby lead to the development of a confidence level for the diagnosis of vascular dementia and to the use of uniform terminology upon which to base evaluation of future intervention programs.

22.

A Case of Cerebral Cysticercosis

MASATOMO KIMURA, KUNIYASU SAKATANI and SHIGEO HASHIMOTO (Osaka, Japan)

Neurocysticercosis is a rare parasitic infection of the central nervous system in most developed countries. Although some sporadic cases have been encountered in Japan, all patients were visitors, immigrants, or Japanese returning from endemic areas. We present a case of cerebral parenchymal neurocysticercosis of a 26-year-old female third generation Japanese visiting Japan from Brazil. The patient was born and grew up in Brazil. She came to Japan in August, 1992 and started to suffer from intermittent headache and nausea in early October. Since she experienced an episode of a convulsion of both upper extremities, she consulted a doctor. There were no other neurological or general

https://doi.org/10.1017/S0317167100049106 Published online by Cambridge University Press

medical symptoms. Her past history did not include tapeworm infestation. On admission, physical examination was normal except for accelerated tendon reflex. A CT scan of the head revealed small high density spots in the right frontal cortices and a low density area with ring enhancement in the parietal lobe. Serological test for cysticercus was positive, and the diagnosis of cerebral cysticercosis was made. The parietal lesion was surgically removed. The parasite was histologically seen in the center of the lesion. It had a spiral folded body and a scolex with suckers and hooks which are characteristic of cysticercus. Granulation tissue surrounded the parasite. Marked lymphocyte and plasma cell infiltration was seen in the middle and outer zones of the granulation tissue. T lymphocytes were predominant compared with B lymphocytes. Most of the infiltrating plasma cells were positive for IgG. In the cerebral parenchyma next to the granulation tissue, edema was prominent and blood vessels were infiltrated with lymphocytes which were identified as T lymphocytes. In the gray matter, degenerated nerve cells were sporadically detected and many GFAP positive astrocytes were seen. Holzer stain and PTAH stain showed fibrillary astrocytes in the border of the gray matter and white matter. Bodian stain and LFB stain showed no particular change of nerve fibers.

23.

Angiographically Occult Vascular Malformation: A Correlative MR Imaging, Histologic, and Immunochemical Study

F.H. TOMLINSON, O.W. HOUSER, B.W. SCHEITHAUER, T. SUNDT JR., H. OKAZAKI and J.E. PARISI (Rochester, U.S.A.)

The spectrum of angiographically occult vascular malformations includes arteriovenous, venous, and cavernous malformations, as well as capillary telangiectasias. The term "cavernous" has both architectural and histologic connotations referring to a compact pattern of growth, one wherein no intervening brain parenchyma is seen, and to the histology of the vessels which are hyaline and lack specific features of arteries or veins. From 1987 through 1990, 106 patients underwent surgery for cerebral vascular malformations. Of these, 25 satisfied the following study criteria: their lesions were angiographically occult and MR imaging, as well as histologic sections, were available for review. Their ages ranged from 4 to 49 years (mean, 30 years). The male to female ration was 1:2. Two-thirds of the lesions were supratentiorial and all were intraparenchymal. All patients were clinically improved following resection. In 24 of the 25 lesions the vascular channels were histologically cavernous in nature; in one case, inadequate sampling precluded histologic classification. Three of the histologically cavernous lesions demonstrated a purely compact or cavernous pattern, 20 a mixed cavernous and racemose pattern (cavernous pattern predominant in six patients), and one a purely racemose pattern. Thrombosis was present in all but one cavernous lesion; in two-thirds recanalization of thrombus was evident. Six of the cavernous lesions exhibited a minor capillary component. Stains for actin demonstrated no formed muscularis. On the basis of this study, we conclude that: a) histologically cavernous lesions are the commonest form of occult vascular malformation; b) a purely compact or cavernous architectural pattern is uncommon, most lesions showing a partially racemose architecture; c) some histologically cavernous malformations possess a capillary component; d) clinical growth of cavernous malformations may have its basis in intramural thrombosis and subsequent recanalization; e) the T_2 weighted MRI pattern of cavernous malformations varies, the most common being a multifocal hyperintense center surrounded by a hypointense ring; f) the MR pattern reflects the histologic appearance; g) since no thrombosed arterivenous malformations were encountered, such lesions must be rare; h) since the pathophysiologic hallmark of a cavernous lesion is recurrent thrombosis and hemorrhage, a resolving hematoma cannot always be distinguished by MR from a cavernous lesion; i) MR is the examination of choice in evaluating occult vascular malformations; and j) microsurgical excision is a satisfactory method of treatment. We suggest the term "cavernous angioma be based upon the histologic appearance of the vessels and that the somewhat artificial requirement of architectural compactness, which is infrequently fulfilled, be abandoned, at least as far as CNS lesions are concerned.

24.

Ultracytochemical Localisation of Calcium in Cerebral Vessels in Chronic Hypertension

S. NAG (Toronto, Ontario)

Our previous studies have suggested that in hypertension increased cerebrovascular permeability to protein by enhanced pinocytosis could be mediated by increased intra-endothelial calcium fluxes. This ultracytochemical study was undertaken to localize calcium in components of the walls of cerebral vessels of normotensive rats and rats with chronic renal hypertension. Postembedding immunohistochemistry using antisera to rat serum proteins was done to determine which vessels were permeable to protein. Rats were sacrificed at weekly intervals by perfusion of a fixative containing 2.5% glutaraldehyde and 3% potassium pyroantimonate. The latter combines with calcium *in vivo* to form calcium pyroantimonate which is electron-dense.

Electron-dense deposits were observed on the outer plasma membranes of endothelial, smooth muscle and adventitial cells of nonpermeable vessels and in the extracellular spaces of the brains of normotensive and hypertensive rats. Three weeks postsurgery, a reduction in the amount of reaction product was observed in vessel walls and in the extracellular spaces of brains of hypertensive rats. Occasional vessels which were leaking protein showed increased calcium deposits on the outer plasma membrane of cerebral endothelium. However increased intra-endothelial calcium in permeable vessels was a rare finding.

These studies failed to provide unequivocal support for the hypothesis that increased intra-endothelial calcium influx mediates increased permeability in hypertension.

Supported by the Heart and Stroke Foundation of Ontario.

25.

Congenital Axonal Neuropathy: Clinical, Electrophysiological and Morphological Study of Seven Cases

ERIC LALUMIÈRE, MICHEL VANASSE and JEAN MICHAUD (Montréal, Québec)

Congenital neuropathy with prevailing axonal changes is an extremely rare entity. Only two cases have been reported so far. In a retrospective study of 159 cases of early onset neuropathy (1979-1990), we identified seven patients affected by such a neuropathy. In three children, symptoms consisting mainly of hypotonia were already severe at birth and two of them died at 24 days and three months of age respectively. The five surviving patients suffered a severe psychomotor retardation and delay in motor development beginning in the neonatal period. The metabolic investigation was normal. For every patient, brain CT Scan showed cerebral atrophy. All patients had nerve conduction velocities and EMG studies suggestive of axonal involvement.

The morphological evaluation was done on three sural nerve biopsies, five muscular biopsies and different specimens obtained at the autopsy of two patients. The peripheral nerve study showed axonal changes with a variable loss of myelinated fibers, axonal atrophy and secondary myelin remodeling. Unmyelinated fibers were involved to a lesser degree. The muscular biopsies showed neurogenic atrophy of variable severity. The brain, available in only one case, showed non specific and mild changes.

The association of congenital axonal neuropathy and psychomotor retardation represents a distinct clinical entity. The morphological evaluation of the peripheral nervous system is helpful in isolating this entity from the other congenital or early onset neuropathies whose etiology remains elusive.

Titles of Diagnostic Case Presentations

1. **Polymicrogyria with Novel Astrocytic Inclusions**
   T.G. BEACH and M.G. NORMAN (Vancouver, B.C.).
   J.E. GOLDMAN (New York, U.S.A.).

2. **Hyperplasia of Choroid Plexus in Association with Tetrasomy 9p**
   M.G. NORMAN, K. POSKITT and D.K. KALOUSEK (Vancouver, B.C.).

3. **Schwannoma**
   S.A. GEORGANOS and V.J.A. MONTPETIT (Ottawa, Ontario).

4. **Schwannoma with Extensive Pseudoglandular Degenerative Change**
   B. CURRY and D.M. SAWYER (Calgary, Alberta).

5. **Paraganglioma of the Cauda Equina**
   J.B. LAMARCHE (Sherbrooke, Quebec).

6. **Malignant Neuroendocrine Neoplasm**
   D. PASLAWSK and B. REWCASTLE (Calgary, Alberta).

7. **Myopathy with Subsarcolemmal Myofiber Inclusions**
   H. VINTERS (Los Angeles, U.S.A.).

8. **Vacuolar Myopathy in Hypokalemic Periodic Paralysis Secondary to Bartter's Syndrome**
   Y. YUCEL and J.M. BILBAO (Toronto, Ontario).

9. **Localised Hypertrophic Neuropathy**
   B. PEREZ-ORDONEZ and G. DAVIDSON (Toronto, Ontario).

10. **Redundant Nerve Root Syndrome of the Cauda Equina**
    A.H. KOEPPEN, A.C. DICKSON and J.A. MCEVOY (Albany, U.S.A.).

11. **Congenital Axonopathy, Compatible with Bovine Progressive Degenerative Encephalomyelopathy of Brown Swiss Cattle**
    J.M. KWIECIEN, H.R. STAEMPFLI, T. MOK, M. RUNSTEDLER (Guelph, Ontario).
    B. LACH (Ottawa, Ontario).

12. **Fibrolipomatous Hamartoma of Nerve**
    P.E. ROWE, D.G. MUNOZ and R.W. GRAINGER (London, Ontario).

13. **Dysembryoplastic Neuroepithelial Tumour**
    A. RACHAMIMOV-STEMMER, I. MACKENZIE and D. MUNOZ (London, Ontario).